Available online at www.sciencedirect.com
SCIENCE DIRECT
Catalysis Today 115 (2006) 228–234
CATALYSIS TODAY
www.elsevier.com/locate/cattod

Performance of catalytic reactors for the hydrogenation of CO_2 to hydrocarbons

Jun-Sik Kim [a], Sunmook Lee [b,1], Sang-Bong Lee [a], Myoung-Jae Choi [a,b,*], Kyu-Wan Lee [c]

[a] Environment and Resources Group, Korea Research Institute of Chemical Technology, Daejeon 305-600, South Korea
[b] Department of Chemical Engineering, Chungnam National University, Daejeon 305-764, South Korea
[c] Division of Biochemical and Engineering, Yanbian University of Science and Technology, Yanji, Jilin 133000, China

Available online 18 April 2006

Abstract

Fluidized bed and slurry reactors were employed to increase the CO_2 conversion and desirable product selectivity in the direct hydrogenation of CO_2 to hydrocarbons over K-promoted iron catalysts, as it is beneficial for the removal of heat generated due to highly exothermic nature of the reaction. The iron catalysts (Fe-K/Al_2O_3 and Fe-Cu-Al-K) were characterized by BET surface area, CO_2 and H_2 chemisorption, temperature-programmed reduction (TPR), X-ray diffraction (XRD) and temperature-programmed hydrogenation (TPH). The results of TPR and TPH study clearly indicated that co-precipitated Fe-Cu-Al-K catalyst has much higher reducibility and catalytic activity of CO_2 hydrogenation at low temperature than Fe-K/Al_2O_3. The performance of fluidized bed or slurry reactors was superior to that of fixed bed reactor for the CO_2 hydrogenation over Fe-Cu-Al-K catalyst in terms of CO_2 conversion and hydrocarbon productivity. Moreover, light olefins and heavy hydrocarbons were selectively synthesized in fluidized bed and slurry reactors, respectively. The optimum operation conditions and the effects of operating variables on the CO_2 conversion and its product distribution in these catalytic reactors were also discussed.

Keywords: Carbon dioxide; Hydrogenation; Iron catalyst; Fixed bed; Fluidized bed; Slurry reactor

1. Introduction

Increased impact of high concentration of CO_2 in the atmosphere on the environment through the greenhouse effect has been of acute concern to the global community and many efforts have been made to control and reduce this emission. Among other CO_2 utilization concepts, catalytic hydrogenation has recently gained great attention [1–4]. Although this approach has not been accepted as an effective mitigation way due to unresolved problems such as CO_2 free hydrogen source and CO_2 free emission process, it is anticipated that this process is still a promising CO_2 mitigation method. This process is expected to provide solutions with regard to the remaining problems related to an advanced power generation system including gasification, reforming and gas-to-liquid process. Development in the near future is expected due to the great potential to produce clean transportation fuels or valuable chemical feedstocks and to simultaneously mitigate a large amount of CO_2 [5,6].

Catalyst system for the hydrogenation of CO_2 has been developed to obtain more valuable chemical feedstock such as light olefins and liquid hydrocarbons. Direct hydrogenation of carbon dioxide to hydrocarbons has been performed over various kinds of Fe-based catalysts, e.g. K, Cr, Mn and Zn promoted iron catalysts prepared by precipitation or impregnation method [7–10]. Our previous studies reported that impregnated Fe-K/Al_2O_3 and co-precipitated Fe-Cu-Al-K catalysts gave a relatively high CO_2 conversion as well as high selectivity of olefins and long chain hydrocarbons in fixed bed reactors [11–18]. Recently, Fischer–Tropsch synthesis in fluidized bed or three-phase slurry reactors has been extensively investigated [19–25] because of its numerous advantages such as effective removal of heat generated from the exothermic reaction and high productivity of hydrocarbons due to effective contact among the reacting phases with higher heat and mass transfer rate and ease of continuous operation mode compared to the other contacting modes [24–26]. Thus, fluidized bed or slurry reactor can be expected to function as an effective system for the hydrogenation of CO_2.

* Corresponding author. Tel.: +82 42 860 7610; fax: +82 42 861 4245.
E-mail address: mjchoi@krict.re.kr (M.-J. Choi).
[1] Present address: Department of Chemical and Environmental Engineering, Illinois Institute of Technology, 10 West 33rd street, Chicago, IL 60616, USA.

0920-5861/$ – see front matter © 2006 Elsevier B.V. All rights reserved.
doi:10.1016/j.cattod.2006.02.038

In the present study, therefore, fluidized bed and slurry reactor have been employed to increase the CO_2 conversion, hydrocarbon productivity and selectivity toward olefins and long chain hydrocarbons. Prior to the reaction, the iron catalysts (Fe-K/Al_2O_3 and Fe-Cu-Al-K) have been characterized by BET surface area, CO_2 and H_2 chemisorption, temperature-programmed reduction (TPR), X-ray diffraction (XRD) and temperature-programmed hydrogenation (TPH). Effects of operating variables on the CO_2 conversion and its product distribution in the different types of catalytic reactors have been investigated.

2. Experimental

2.1. Catalyst preparation

Fe-K/Al_2O_3 catalyst was prepared by the impregnation of γ-alumina supports (Strem, 200 m^2/g) with aqueous solutions of $Fe(NO_3)_3{\cdot}9H_2O$ and K_2CO_3. The catalyst was homogeneously mixed and dried in a stirred vacuum evaporator at 80 °C and calcined at 500 °C for 12 h. The nominal catalyst compositions were 20Fe:7K:100Al_2O_3 wt%. To study the effect of particle size on the catalytic activity in a fixed bed reactor, a series of catalysts with different particle size (d_p = 0.5, 1.5, 2.5, 5 and 10 mm) were extruded with a PVA binder [17]. Fe-Cu-Al-K catalyst was prepared by precipitation and incipient wetness method [13,14]. The precursor of 100Fe:6Cu:15Al (wt%) was made using co-precipitation method with ammonium hydroxide and homogeneous metal nitrate solution which was made of $Fe(NO_3)_3{\cdot}9H_2O$, $Cu(NO_3)_2{\cdot}3H_2O$ and $Al(NO_3)_3{\cdot}9H_2O$ at pH 6.8. The precipitates were washed with distilled water, and dried at 110 °C for 24 h. Potassium was added to the dried precursor in the form of K_2CO_3 solution (Fe:K = 100:6 wt%) using incipient wetness method. The catalyst was dried at 110 °C for 48 h and calcined at 450 °C for 6 h. The crushed and sieved catalysts were loaded in a fixed bed, fluidized bed, and slurry reactor.

2.2. Catalyst characterization

X-ray diffractometer was used to examine the crystallinity of the catalysts. The spectra were scanned at a rate of 1.0/min on a Rigaku 2155D6 with a Cu Kα X-ray source (40 kV, 40 mA). The surface area and pore volume of the catalysts were measured by BET using Micrometrics ASAP-2400. The physical and chemical properties of catalysts are given in Table 1. TPR experiments were carried out in a temperature controllable quartz tube reactor equipped with a thermal conductivity detector (TCD) at different heating rates of 5, 10 and 20 °C/min. The uptake amount of CO_2 and H_2 was measured at 35 °C using Micrometrics ASAP-2020. To compare the catalytic activity in terms of the rate of CO_2 conversion corresponding to reaction temperature, TPH of CO_2 study was carried out in a micro-fixed bed reactor (T = 200–400 °C, 0.1 °C/min, SV = 500 ml/g_{cat} h, P = 1 MPa). The reactor was filled with catalyst diluted with quartz sand in a weight ratio of catalyst to quartz sand of 1/5.

2.3. Catalytic reaction

In this work, to evaluate the reactor performance, three types of catalytic reactors were employed for the CO_2 hydrogenation. A schematic diagram of the bench-scale fixed bed (0.024 m i.d. × 0.6 m high), fluidized bed (0.024 m i.d. × 0.6 m high) and slurry reactor (0.05 m i.d. × 0.15 m high) is illustrated in Fig. 1. In the slurry reaction system, squalane was used as a slurry medium and all experiments were carried out at a stirring speed of 700 rpm without external transport limitations [21]. Details of each reaction system were described in the previous papers [13–17]. Flow rates of gases (CO_2, H_2, Ar or N_2) were controlled by mass flow controller (MFC, Brooks Co.). Reaction temperature was controlled within the range of 275–325 °C using an electric heater and temperature control system. The temperatures at the heater surface as well as in the reactor bulk were measured by K-type thermocouples. Reaction pressure was regulated by back pressure regulator (BPR, Tescom Co.) in the range of 1.0–2.5 MPa and measured by pressure sensors. Oil products were passed through the gas/liquid separator and collected in a condenser connected to a heat exchanger (0 °C) and then were weighed and analyzed by GC equipped with FID (SPB-1 column). Uncondensed gases and light hydrocarbons (CO_2, CO and C_1–C_6) were analyzed with GC-TCD (Carbosphere column) and FID (Poraplot-Q column). The exit gases were measured with wet gas meter. The CO_2 conversion (X_{CO_2}), CO selectivity (S_{CO}) and CH_4 selectivity (S_{CH_4}) were obtained from the GC-TCD data, in which Ar is the internal standard gas.

3. Results and discussion

3.1. Catalyst characterization

In this study, two kinds of K-promoted iron catalysts were prepared by impregnation method (Fe-K/Al_2O_3) and co-precipitation method (Fe-Cu-Al-K). The physical and chemical properties of the iron catalysts are summarized in Table 1. Alumina supported Fe-K catalyst shows much higher uptake amounts of CO_2 and H_2 than those of co-precipitated Fe-Cu-Al-K catalyst. This can be attributed to the high surface area of Fe-K/Al_2O_3 catalysts, which depends upon the compositional nature of the alumina supports [11,13]. The catalyst reducibility

Table 1
Physical and chemical properties of the iron catalysts

Catalysts	Composition (wt%)	BET surface area (m^2/g)	CO_2 uptake (μmol/g)	H_2 uptake (μmol/g)
Fe-K/Al_2O_3	20:7:100	124.5	375.5	13.7
Fe-Cu-Al-K	100:6.0:14.7:6.2	97.1	279.6	8.4

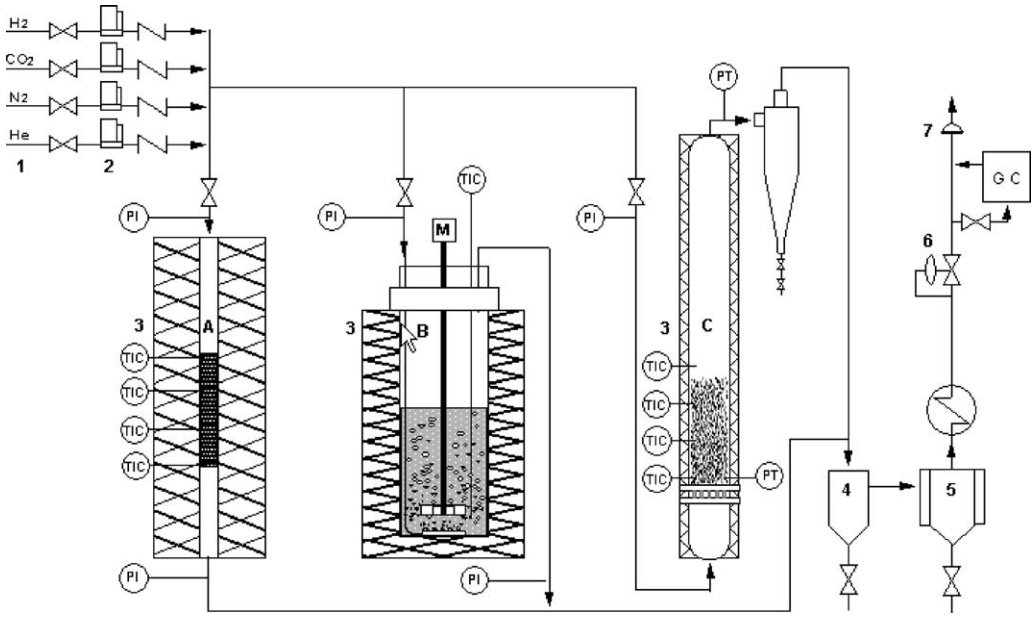

Fig. 1. Schematic diagram of experimental apparatus: (A) fixed bed reactor, (B) slurry reactor, (C) fluidized bed reactor, (1) feed gas cylinders, (2) mass flow controller, (3) electric heater, (4) G/L separator, (5) condenser, (6) BPR and (7) wet gas meter.

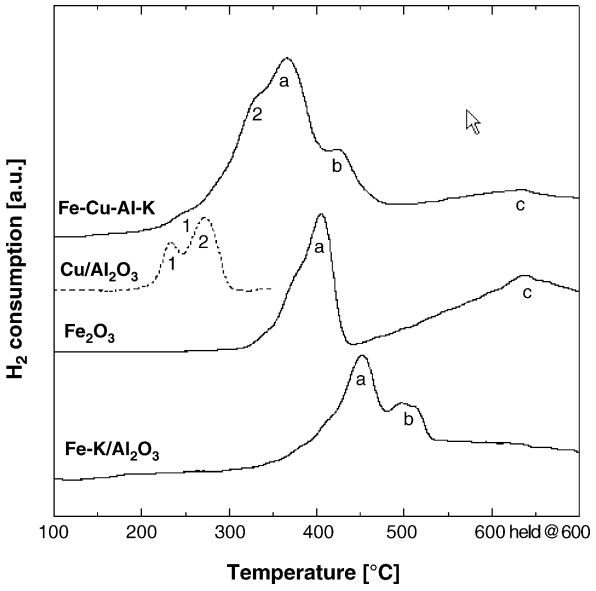

Fig. 2. H_2-TPR patterns of the iron catalysts (a) $Fe_2O_3 \rightarrow Fe_3O_4$, (b) $Fe_3O_4 \rightarrow FeO$, (c) $FeO \rightarrow Fe$, (1) $CuO \rightarrow Cu_2O$ and (2) $Cu_2O \rightarrow Cu$.

and metal–support interactions were investigated with TPR experiments. Fig. 2 shows the H_2-TPR patterns of the iron catalysts. For the Fe_2O_3 sample, only two reduction peaks appeared in the TPR profile. The low temperature peaks correspond to the reduction of (a) Fe_2O_3 to Fe_3O_4, and high temperature peaks to the reduction of (c) Fe_3O_4 to α-Fe. However, in the case of Fe-K/Al_2O_3 and Fe-Cu-Al-K catalysts, the middle peaks are observed in the TPR profiles. The middle peaks may be attributed to the transformation of (b) Fe_3O_4 to FeO, which appears to be influenced by the metal–support interactions resulting from alkali metal introduction. This phenomenon is in good agreement with the results of previous study [12], in which they reported the three-step reduction mechanism of alkali ion-exchanged Y-zeolite iron catalysts. The TPR profile of Cu/Al_2O_3 shows two reduction peaks at low temperatures (235 and 275 °C), corresponding to the reduction of (1) CuO to Cu_2O and (2) Cu_2O to Cu, respectively. The Cu component remarkably enhances the reducibility of Fe_2O_3, which can be clearly confirmed by the stronger signal intensity in the TPR of Fe-Cu-Al-K catalysts. The TPR profiles of Fe-K/Al_2O_3 catalysts, however, occurred at a much higher temperature (458 °C) than that of Fe_2O_3 (407 °C). The difference in reducibility between Fe-K/Al_2O_3 and Fe-Cu-Al-K catalyst could be explained by the activation energy (E_a). Table 2 shows the activation energy for the reduction of Fe_2O_3 to Fe_3O_4 using Ozawa method [27], which was obtained based on the shift of the maximum deflection temperature (T_m) upon changing the heating rate. The activation energy of reduction was lower

Table 2
Activation energy for the reduction of Fe_2O_3 to Fe_3O_4 on the Fe catalysts

Catalysts	T_m (°C)			E_a (kJ/mol)	r (−)
	ϕ = 5 °C/min	ϕ = 10 °C/min	ϕ = 20 °C/min		
Fe-K/Al_2O_3	441	492	555	56.9	0.997
Fe-Cu-Al-K	323	370	410	48.9	0.995

E_a is calculated by Ozawa method ($\log \phi = E_a/RT_m$) and the symbol r is the linear correlation coefficient.

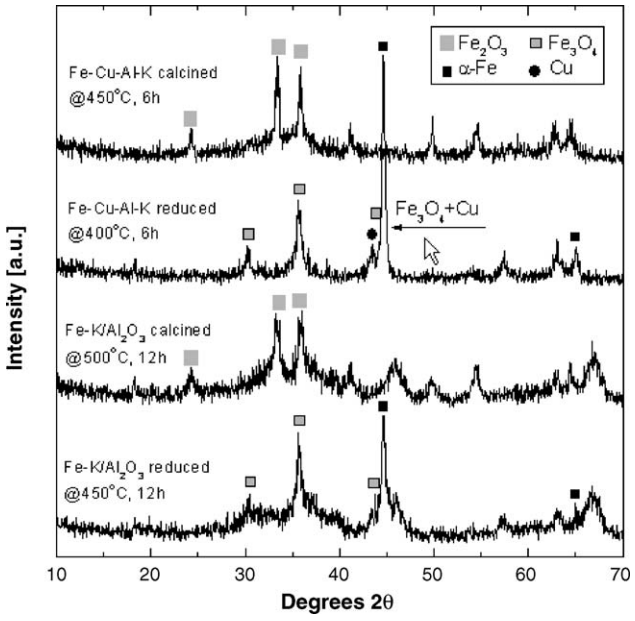

Fig. 3. XRD patterns of the iron catalysts.

with Fe-Cu-Al-K catalyst compared to that without Cu component. The E_a obtained for the reduction of Fe_2O_3 in Fe-K/Al_2O_3 and Fe-Cu-Al-K was 56.9 and 48.9 kJ/mol, respectively.

Fig. 3 shows the XRD patterns of Fe-K/Al_2O_3 and Fe-Cu-K-Al catalysts. After calcination under air, iron component assigned predominantly to Fe_2O_3 was observed. And the iron component, Fe_2O_3, was transformed to Fe_3O_4 and α-Fe by H_2-reduction. The reduction mechanism of Fe_2O_3 from TPR profiles was partly confirmed by XRD measurements. However, no XRD peaks corresponding to FeO were clearly observed. This is ascribed to the thermodynamically metastable FeO bulk phase compared to either Fe_3O_4 or α-Fe [28]. The XRD measurements clearly indicate that Fe-Cu-Al-K shows a greater reduction from Fe_2O_3 to Fe_3O_4 compared to Fe-K/Al_2O catalysts.

To evaluate catalytic activity as a function of reaction temperature, TPH experiment was carried out in the micro-fixed bed reactor. Prior to the increase of reaction temperature, the reaction was kept at 200 °C for 12 h to allow the reaction to reach pseudo steady-state in terms of CO_2 conversion (X_{CO_2}). The reaction temperature of CO_2 hydrogenation was increased at a heating rate of 0.1 °C/min. The results of TPH are shown in Fig. 4. In this figure, X_{CO_2} gradually increases with increasing temperature and reaches a plateau while

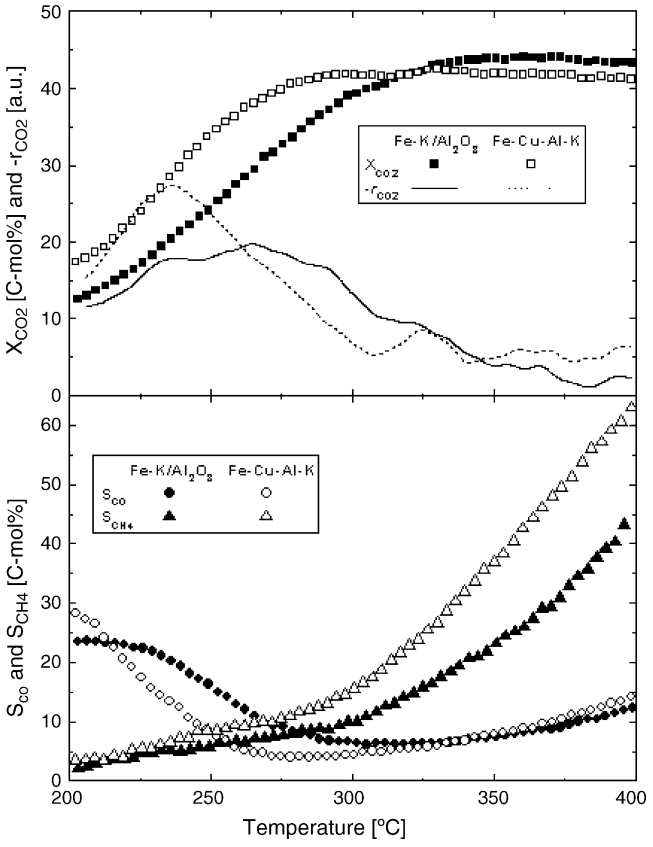

Fig. 4. TPH profiles of X_{CO_2}, S_{CO} and S_{CH_4} in the micro-fixed bed reactor (SV = 500 ml/g_{cat} h, P = 1 MPa, H_2/CO_2 = 3).

further increasing the reaction temperature, whereas the selectivity of CO (S_{CO}) decreases and above a certain temperature (300 °C) no further decrease was observed. The maximum temperature of CO_2 conversion rate ($-r_{CO_2}$) of Fe-K/Al_2O_3 and Fe-Cu-Al-K was observed at 265 and 235 °C, respectively, which is consistent with the difference of reduction temperature between Fe-K/Al_2O_3 and Fe-Cu-Al-K in the TPR profiles. The results of TPH study clearly indicate that co-precipitated Fe-Cu-Al-K catalyst has much higher catalytic activity at low temperature in the CO_2 hydrogenation than that of Fe-K/Al_2O_3. It is interesting to note that the product selectivity of both catalysts shows almost the same distribution at the same level of CO_2 conversion in spite of different reaction temperatures as can be verified in Table 3. On the contrary, Fe-K/Al_2O_3 catalyst shows a more stable activity at high temperature (>300 °C) with relatively high X_{CO_2} and lower S_{CH_4} compared to those of Fe-Cu-Al-K

Table 3
Results of the CO_2 conversion and product selectivity obtained from TPH

Catalysts	T (°C)	X_{CO_2} (%)	S_{CO} (%)	Hydrocarbon distribution (C-mol%)								O/O + P, C_2–C_4 (%)
				C_1	$C_2^=$	C_2	$C_3^=$	C_3	$C_4^=$	C_4	$\geq C_5$[a]	
Fe-K/Al_2O_3	300	38.9	6.5	9.6	5.4	2.7	16.8	2.3	13.2	2.7	47.3	82.1
Fe-Cu-Al-K	275	39.8	4.2	10.1	5.2	2.8	15.8	2.1	11.3	2.6	50.1	81.2

Reaction conditions: micro-fixed bed reactor, SV = 500 ml/g_{cat} h, P = 1 MPa, H_2/CO_2 = 3.
[a] Oxygenate compounds included in $\geq C_5$ fraction.

catalyst since the alumina support for the CO_2 hydrogenation provides relatively high dispersion of the catalytic component and a high degree of thermal stability [11].

3.2. CO_2 hydrogenation in the different types of reactors

Fixed bed reactors are the most widely used reactor type for gas phase reactants in the production of large-scale basic chemicals and intermediates [29]. In the case of fixed bed reactors for the CO_2 hydrogenation to hydrocarbons, however, the productivity of hydrocarbon and the selectivity of a desirable product did not show reasonable levels to develop a commercial process because the reaction has intrinsic limitations on the diffusion and heat transfer in fixed beds [12–15]. Due to pressure drop constraints with small particle size, in most fixed bed processes the beds are filled with catalysts with diameters above 1 mm, which can limit the overall reaction rate because of the intraparticle diffusion [29]. Fig. 5 shows the effect of particle size on the X_{CO_2} and S_{CO} over Fe-K/Al_2O_3 catalyst in the fixed bed reactor. X_{CO_2} greatly decreases and S_{CO} increases with increasing the particle sizes. This can be ascribed to the fact that the increase of S_{CO} is limited by external ($d_p > 2.5$ mm, $d_r/d_p < 10$) and intraparticle ($d_p < 2.5$ mm, $d_r/d_p > 10$) diffusion in the consecutive reaction. It has been reported that the hydrogenation of CO_2 proceeds via a two-step mechanism [3,8]. In the reverse water gas shift reaction ($\Delta_R H^0 = 38$ kJ/mol), CO_2 converted to CO, which is an intermediate product in a consecutive reaction, and the CO is hydrogenated to the organic products in the F–T reaction ($\Delta_R H^0 = -166$ kJ/mol). On the other hand, pressure drop per unit length ($\Delta P/L$) exponentially increased with a small particle size ($d_p < 1$ mm) as shown in Fig. 5.

In this study, influences of catalyst size in the fixed bed were investigated using impregnated Fe-K/Al_2O_3 catalyst since it is more easily manufactured as a catalyst pellet than co-precipitated Fe-Cu-Al-K catalyst. It has been reported in the preparation of heterogeneous catalysts that the support should enable the production of a large shaped particle composed of very small, easily sintered crystals of active phase which are prevented from coalescing by being separated from the support component [30]. Recently, the high attrition-resistant supported iron catalysts for use in F–T synthesis have been developed because of the high attrition rate of conventional precipitated iron catalysts. However, alumina support catalysts did not appear to be as attrition resistant as silica containing catalysts since the catalyst fracture occurred during the CSTR run [31]. Moreover, it has been pointed out that the activity of supported iron catalysts is much lower and the methane selectivity is unacceptably higher than those of precipitated iron catalysts [32]. Similar results for the CO_2 hydrogenation using supported Fe-K/Al_2O_3 catalyst were observed in the fluidized bed and slurry reactor. The activity of the Fe-K/Al_2O_3 catalyst was below 20% X_{CO_2} and CO selectivity was above 50%. Since the activity of Fe-K/Al_2O_3 catalyst is not reasonable to explain the performance of fluidized bed or slurry reaction, the reactor performance using Fe-K/Al_2O_3 catalyst is not discussed further.

To compare the performance of different types of reactors, co-precipitated Fe-Cu-Al-K catalysts were employed with crushed forms for each reaction. The sizes of Fe-Cu-Al-K catalysts for the fixed bed, fluidized bed and slurry reactor were in the range of d_p = 350–850 μm, d_p = 75–90 μm and d_p = 45–75 μm, respectively. The axial temperature distributions of CO_2 hydrogenation in different types of reactors are shown in Fig. 6. In case of fixed bed reactors, there is a 'hot spot' occurring at the inlet of gaseous reactants for CO_2 hydrogenation, meaning a highly exothermic reaction as well as F–T synthesis. However, this can be overcome by employing

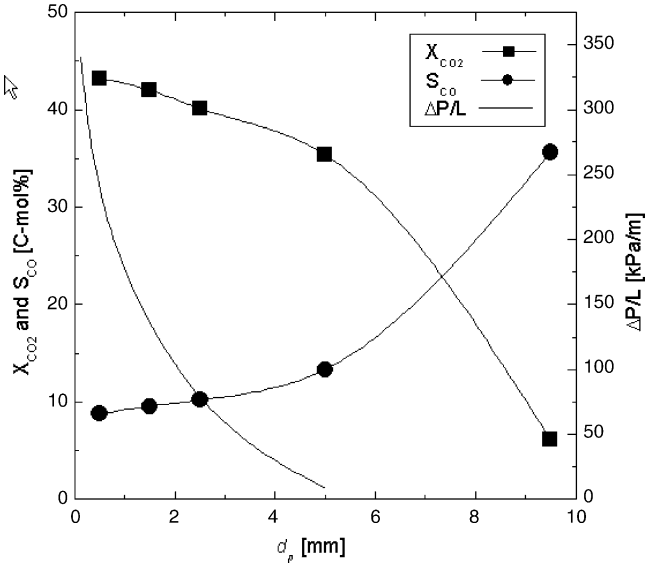

Fig. 5. Effect of particle size on the X_{CO_2}, S_{CO} and pressure drop in the fixed bed reactor (Cat. = Fe-K/Al_2O_3, SV = 2000 ml/g_{cat} h, T = 315 °C, P = 1 MPa, H_2/CO_2 = 3).

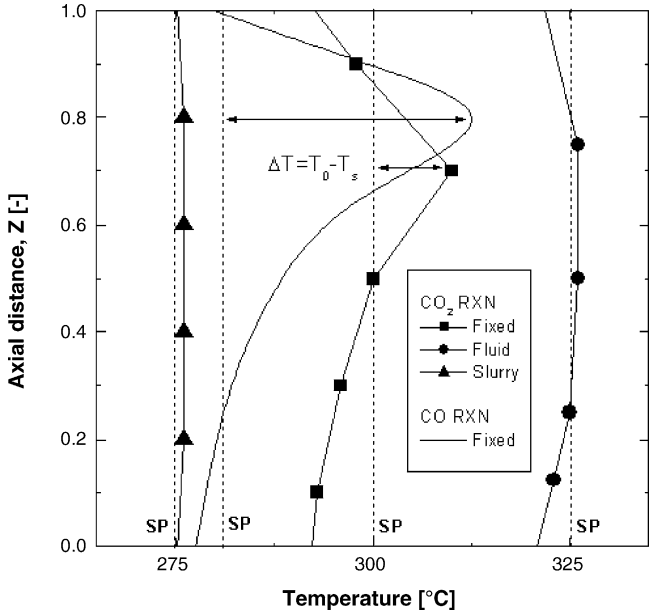

Fig. 6. Axial temperature distribution of CO_2 hydrogenation in the different type of reactor (Cat. = Fe-Cu-Al-K, SV = 2000 ml/g_{cat} h, P = 1 MPa, H_2/CO_2 = 3).

fluidized bed or slurry reactors, due to their excellent heat transfer rate. There is a 2 °C of temperature difference (ΔT) in the reactor bulk region of the fluidized bed or slurry reactor. The fixed bed reactor has a limitation of heat removal which could accelerate the deactivation of catalyst and production of undesired CH_4, Therefore, the fluidized bed reactor was used for the high temperature reaction toward light hydrocarbons whereas the slurry reactor was used for the production of heavy hydrocarbons at low temperature. The performance of fluidized bed or slurry reactor was compared with that of fixed bed reactor.

In our previous studies [13–18], effects of operating variables (reaction temperature, pressure, gas velocity, space velocity, H_2/CO_2 ratio, etc.) on the product selectivity over K-promoted iron catalysts in the different types of reactors have been investigated. Effects of operating variables on the product selectivity in the CO_2 hydrogenation were similar to those in the F–T synthesis, whereas light hydrocarbons and olefins selectivities were found to be much higher in the CO_2 hydrogenation than those in the F–T synthesis. Molecular weight distribution of hydrocarbons as a function of the carbon number is shown in Fig. 7. From the weight of liquid hydrocarbons in the range of carbon number (Nc) C_{10}–C_{20}, chain growth probability (α) was calculated to be 0.85, 0.92 and 0.71 in the fixed bed, slurry reactor and fluidized bed, respectively. This result can be explained such that the selection of reactor type enables the selective synthesis of hydrocarbons since the difference of α-value is attributed to the reaction temperature which is acceptable for the rate of heat removal in each type of reactor. The high α-value of CO_2 hydrogenation in the slurry reactor is comparable to that reported for F–T synthesis using alkali promoted Fe catalysts in CSTR (α = 0.92–0.95 at 260 °C) [33]. Moreover, the olefin-(1) content in linear hydrocarbons was much higher at high temperature (325 °C) in the fluidized bed than that in the fixed bed or slurry reactor as shown in Fig. 8. For olefins production in modified F–T process, Hu [34] pointed out that available approaches are changes in operating conditions, reactor design and development of high selective catalysts. From the experimental results of previous studies [15–18], it is possible to combine the optimum process parameter for the selective synthesis toward light olefins or heavy paraffins obtained with different types of reactors. Influences of process parameters on the product distribution with different types of reactors are shown in Fig. 9.

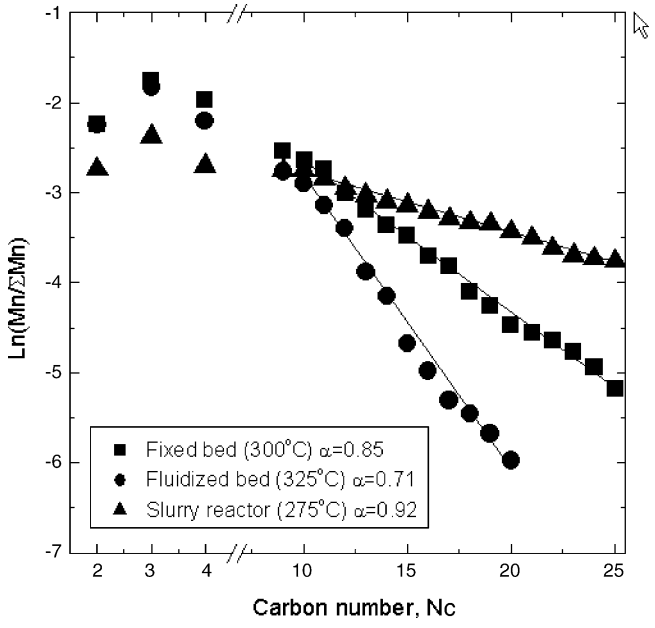

Fig. 7. Molecular weight distribution of hydrocarbons as a function of the carbon number (Cat. = Fe-Cu-Al-K, SV = 2000 ml/g_{cat} h, P = 1 MPa, H_2/CO_2 = 3).

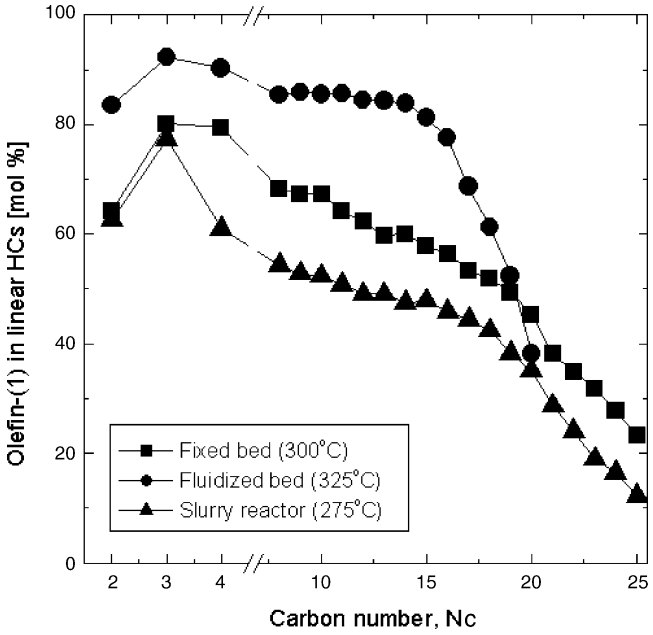

Fig. 8. Olefin-(1) content in linear hydrocarbons as a function of the carbon number (Cat. = Fe-Cu-Al-K, SV = 2000 ml/g_{cat} h, P = 1 MPa, H_2/CO_2 = 3).

The results of the CO_2 conversion and product selectivity obtained with different types of reactors are summarized in Table 4. The productivity of reactor in terms of space-time-yield (STY) was obtained in the order of fluidized bed

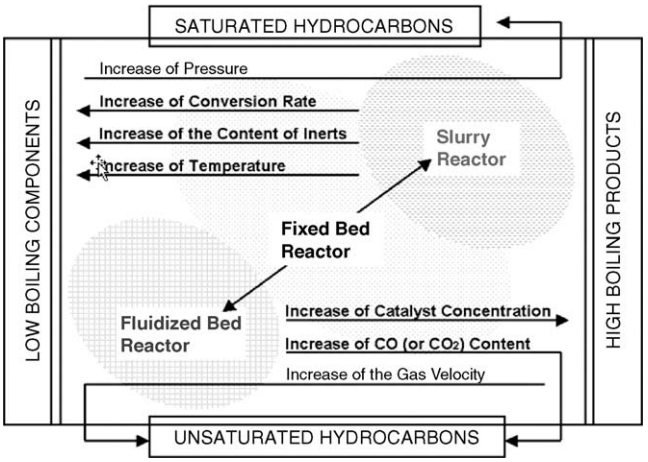

Fig. 9. Influence of the process parameters in the different type of reactor on the product distribution [34].

Table 4
Results of the CO_2 conversion and product selectivity obtained with different types of reactors

Reactor types	T (°C)	X_{CO_2} (%)	STY (mmol/g_{cat} h)	S_{CO} (%)	Hydrocarbon distribution (C-mol%)								O/O + P, C_2–C_4 (%)
					C_1	$C_2^=$	C_2	$C_3^=$	C_3	$C_4^=$	C_4	$\geq C_5$[a]	
Fixed bed	300	35.6	31.8	9.6	10.9	5.8	3.2	11.6	2.9	9.3	2.4	53.9	75.9
Fluidized bed	300	46.8	41.8	8.2	9.8	7.5	2.1	13.7	1.3	8.8	1.2	55.6	86.7
Slurry	300	39.4	35.2	7.6	8.3	3.7	1.7	6.3	1.5	3.7	1.9	72.9	72.9
Fluidized bed	325	48.9	43.7	8.8	12.2	7.8	1.6	14.1	1.2	8.2	0.8	54.1	89.3
Slurry	275	32.4	28.9	7.4	5.8	3.5	2.1	5.6	1.6	3.3	2.1	76.0	68.1

Reaction conditions: Cat.: Fe-Cu-Al-K, SV = 2000 ml/g_{cat} h, P = 1 MPa, H_2/CO_2 = 3; STY, space-time-yield is expressed in mmol of CO_2 converted/g_{cat} h.
[a] Oxygenate compounds included in $\geq C_5$ fraction.

(STY = 41.8) > slurry reactor (STY = 35.2) > fixed bed reactor (STY = 31.8) at 300 °C. The olefins selectivity (O/O + P) exhibited much higher values (89.3%) at 325 °C in the fluidized bed reactor than those in the other types of reactors, whereas liquid hydrocarbons ($\geq C_5$) exhibited much higher values (76.0%) in the slurry reactor at 275 °C than those in the other types of reactors. It is noted that the selectivity of oxygenate compounds exhibited much higher values in the fluidized bed reactor (28.8%) than that in the fixed (3.5%) or slurry reactor (3.8%). In the oxygenate compounds, ethanol was predominantly formed (45 wt%) in the fluidized bed.

4. Conclusions

For the direct hydrogenation of CO_2 to hydrocarbons, fluidized bed and slurry reactors with iron catalysts were employed as alternatives to fixed bed reactors to increase the CO_2 conversion and desirable product selectivity due to their effective removal of heat generated during the reaction, which is highly exothermic. Two types of catalysts (Fe-K/Al_2O_3 and Fe-Cu-Al-K) were prepared and tested, and it has been found that co-precipitated Fe-Cu-Al-K catalyst had much higher reducibility and catalytic activity of CO_2 hydrogenation at low temperature from the results of TPR and TPH study.

The productivity of reactor using Fe-Cu-Al-K catalysts was obtained in the order of fluidized bed (STY = 41.8) > slurry reactor (STY = 35.2) > fixed bed reactor (STY = 31.8). The olefins selectivity (O/O + P) exhibited much higher values (89.3%) in the fluidized bed reactor than those in the other types of reactors, whereas liquid hydrocarbons ($\geq C_5$) exhibited much higher values (76.0%) in the slurry reactor than those in the other types of reactors. These results indicate that the fluidized bed and slurry reactors for the direct hydrogenation processes of CO_2 to hydrocarbons over Fe-Cu-Al-K catalysts showed better catalytic performance than that of fixed bed reactor in view of CO_2 conversion and products selectivity.

Acknowledgements

The authors gratefully appreciate financial support of this work by the clean energy research program under the Korea Energy Management Corporation (KEMCO). We wish to thank Dr. Ki-Won Jun (KRICT) for scientific comments.

References

[1] X. Xiaoding, J.A. Moulijin, Energy Fuels 10 (1996) 350.
[2] K. Tomishige, K. Fujimoto, Catal. Surveys Jpn. 2 (1998) 3.
[3] T. Riedel, G. Schaub, K.W. Jun, K.W. Lee, Ind. Eng. Chem. Res. 40 (2001) 1355.
[4] Y. Zhang, G. Jacobs, D.E. Sparks, M.E. Dry, B.H. Davis, Catal. Today 71 (2002) 411.
[5] T. Furusawa, A. Tsutsumi, Appl. Catal. A 278 (2005) 195.
[6] M.J. Prins, K.J. Ptasinski, F.J.J.G. Janssen, Fuel Process. Technol. 86 (2004) 375.
[7] J. Barrault, C. Forquy, J.C. Menezo, R. Maurel, React. Kinet. Catal. Lett. 17 (1981) 373.
[8] M.D. Lee, J.F. Lee, C.S. Chang, Bull. Chem. Soc. Jpn. 62 (1989) 2756.
[9] H. Ando, Q. Xu, M. Fujiwara, Y. Matsumura, Y. Souma, Catal. Today 45 (1998) 229.
[10] L. Xu, Q. Wang, D. Liang, X. Wang, L. Lin, W. Cui, Y. Xu, Appl. Catal. A 173 (1998) 19.
[11] P.H. Choi, K.W. Jun, S.J. Lee, M.J. Choi, K.W. Lee, Catal. Lett. 40 (1996) 115.
[12] S.S. Nam, H. Kim, G. Kishan, M.J. Choi, K.W. Lee, Appl. Catal. A 179 (1999) 155.
[13] S.R. Yan, K.W. Jun, J.S. Hong, M.J. Choi, K.W. Lee, Appl. Catal. A 194 (2000) 63.
[14] J.S. Hong, J.S. Hwang, K.W. Jun, J.C. Sur, K.W. Lee, Appl. Catal. A 218 (2001) 53.
[15] M.J. Choi, J.S. Kim, H.K. Kim, Y. Kang, S.B. Lee, K.W. Lee, Korean J. Chem. Eng. 18 (2001) 646.
[16] J.S. Kim, S.B. Lee, M.C. Kang, K.W. Lee, M.J. Choi, Y. Kang, Korean J. Chem. Eng. 20 (2003) 967.
[17] S.B. Lee, J.S. Kim, W.Y. Lee, K.W. Lee, M.J. Choi, Stud. Surf. Sci. Catal. 153 (2004) 73.
[18] J.S. Kim, S.B. Lee, M.J. Choi, Y. Kang, K.W. Lee, Stud. Surf. Sci. Catal. 153 (2004) 177.
[19] M.E. Dry, Chemtech (December) (1982) 744.
[20] B. Jager, R. Espinoza, Catal. Today 23 (1995) 17.
[21] A.P. Raje, B.H. Davis, Catal. Today 36 (1997) 335.
[22] D.B. Bukur, X. Lang, Ind. Eng. Chem. Res. 38 (1999) 3270.
[23] A.P. Steynberg, R.L. Espinoza, B. Jager, A.C. Vosloo, Appl. Catal. A 186 (1999) 41.
[24] S.T. Sie, R. Krishna, Appl. Catal. A 186 (1999) 55.
[25] E. Sanders, S. Ledakowicz, W.D. Deckwer, Can. J. Chem. Eng. 64 (1986) 133.
[26] S.D. Kim, Y. Kang, Chem. Eng. Sci. 52 (1997) 3639.
[27] T. Ozawa, J. Therm. Anal. 5 (1973) 563.
[28] A.J.H.M. Koch, H.M. Fortuin, J.W. Geos, J. Catal. 96 (1985) 261.
[29] P. Andrigo, R. Bagatin, G. Pagani, Catal. Today 52 (1999) 197.
[30] M. Campanati, G. Fornasari, A. Vaccari, Catal. Today 77 (2003) 299.
[31] R.J. O'Brien, L. Xu, S. Bao, A. Raje, B.H. Davis, Appl. Catal. A 196 (2000) 173.
[32] J. Xu, C.H. Bartholomew, J. Phys. Chem. B 109 (2005) 2392.
[33] D.B. Bukur, C. Sivaraj, Appl. Catal. A 231 (2002) 201.
[34] Y.C. Hu, Hydrocarbon Process. (May) (1983) 88.